



Title	Charge trapping properties in TiO <sub>2</sub> /HfSiO <sub>2</sub> /SiO <sub>2</sub> gate stacks probed by scanning capacitance microscopy
Author(s)	Naitou, Y.; Arimura, H.; Kitano, N. et al.
Citation	Applied Physics Letters. 2008, 92(1), p. 012112
Version Type	VoR
URL	<a href="https://hdl.handle.net/11094/85486">https://hdl.handle.net/11094/85486</a>
rights	This article may be downloaded for personal use only. Any other use requires prior permission of the author and AIP Publishing. This article appeared in Appl. Phys. Lett. and may be found at <a href="https://doi.org/10.1063/1.2828863">https://doi.org/10.1063/1.2828863</a> .
Note	

*The University of Osaka Institutional Knowledge Archive : OUKA*

<https://ir.library.osaka-u.ac.jp/>

The University of Osaka

# Charge trapping properties in $\text{TiO}_2 / \text{HfSiO} / \text{SiO}_2$ gate stacks probed by scanning capacitance microscopy

Cite as: Appl. Phys. Lett. **92**, 012112 (2008); <https://doi.org/10.1063/1.2828863>

Submitted: 30 October 2007 • Accepted: 05 December 2007 • Published Online: 07 January 2008

Y. Naitou, H. Arimura, N. Kitano, et al.



View Online



Export Citation

## ARTICLES YOU MAY BE INTERESTED IN

[Contrast distortion induced by modulation voltage in scanning capacitance microscopy](#)

Applied Physics Letters **101**, 083503 (2012); <https://doi.org/10.1063/1.4747319>

[Spatial fluctuation of dielectric properties in Hf-based high- \$k\$  gate films studied by scanning capacitance microscopy](#)

Applied Physics Letters **87**, 252908 (2005); <https://doi.org/10.1063/1.2149222>

[Scanning capacitance microscopy](#)

Journal of Applied Physics **57**, 1437 (1985); <https://doi.org/10.1063/1.334506>

 QBLOX



1 qubit

Shorten Setup Time

**Auto-Calibration**  
**More Qubits**

Fully-integrated

**Quantum Control Stacks**  
**Ultrastable DC to 18.5 GHz**  
Synchronized <<1 ns  
Ultralow noise



100s qubits

[visit our website >](#)

# Charge trapping properties in $\text{TiO}_2/\text{HfSiO}/\text{SiO}_2$ gate stacks probed by scanning capacitance microscopy

Y. Naitou,<sup>a)</sup> H. Arimura, N. Kitano,<sup>b)</sup> and S. Horie

*Graduate School of Engineering, Osaka University, 2-1 Yamadaoka, Suita, Osaka 565-0871, Japan*

T. Minami and M. Kosuda

*Canon Anelva Corporation, 2-5-1 Kurigi, Asao-ku, Kawasaki 215-8550, Japan*

H. Ogiso

*Advanced Manufacturing Research Institute, National Institute of Advanced Industrial Science and Technology (AIST), 1-2-1 Namiki, Tsukuba, Ibaraki 305-8564, Japan*

T. Hosoi, T. Shimura, and H. Watanabe

*Graduate School of Engineering, Osaka University, 2-1 Yamadaoka, Suita, Osaka 565-0871, Japan*

(Received 30 October 2007; accepted 5 December 2007; published online 7 January 2008)

The charge-trapping properties of the high-permittivity titanium oxide–hafnium silicate–silicon dioxide ( $\text{TiO}_2/\text{HfSiO}/\text{SiO}_2$ ) gate stacks have been studied using scanning capacitance microscopy. From the bias stress examination of the gate stacks, we concluded that there were electron traps within the films, and these trap densities increased with an increase in the oxidation temperature used for the fabrication of  $\text{TiO}_2$  top dielectrics. Furthermore, we found that the distribution of these charged defects was inhomogeneous within the gate stacks. These results are attributed to Ti diffusion through the dielectric layers, which caused electrical defects within the gate stacks.

© 2008 American Institute of Physics. [DOI: 10.1063/1.2828863]

The continuous downscaling of Si-based metal-oxide-semiconductor field effect transistors (MOSFETs) will soon require substitutes for conventional  $\text{SiO}_2$  as the gate dielectrics. High permittivity (high- $k$ ) metal oxides are expected to maintain the physical thickness of gate dielectrics, enabling the gate leakage current to be suppressed.<sup>1</sup> Among the several candidates for high- $k$  materials, hafnium oxide ( $\text{HfO}_2$ ) and its silicate ( $\text{HfSiO}$ ) films are expected to be promising materials.<sup>2</sup> However, silicate films have lower dielectric constants compared with oxide films. Therefore, an effective approach seems to be to mix the silicate films with other high- $k$  materials to further improve the properties of the gate dielectrics. For this purpose, titanium oxide ( $\text{TiO}_2$ ) and its composite or layered structure are attractive because of its very high dielectric constant (50–170).<sup>3</sup> To confirm the reliability of high- $k$  gate stacks, charged defects within high- $k$  films should be closely investigated because they induce threshold voltage instabilities or trap-assisted leakage current.<sup>4</sup> In the present study, the charge-trapping properties of  $\text{TiO}_2/\text{HfSiO}/\text{SiO}_2$  gate stacks and their dependence on the preparation process were characterized through scanning capacitance microscopy (SCM) measurements.

The sample preparation procedure was as follows. After a 1.4-nm-thick  $\text{SiO}_2$  underlayer had been formed on a  $p$ -Si(100) substrate by conventional rapid thermal oxidation, ultrathin 0.5-nm-thick metal Hf layers were deposited by low-damage sputtering on the  $\text{SiO}_2/\text{Si}$  maintained at room temperature. The  $\text{HfSiO}$  layer was then formed by utilizing a solid phase interface reaction between the metal Hf layer and

$\text{SiO}_2$  underlayer by annealing in an oxygen partial pressure ( $10^{-3}$  Torr) ambient at 850 °C for 1 min.<sup>5</sup> Then, 0.5-nm-thick metal Ti layers were deposited on the  $\text{HfSiO}$  layer and oxidized by annealing in an oxygen partial pressure ( $10^{-3}$  Torr) ambient at 400 °C (sample 2) and 600 °C (sample 3) for 1 min.<sup>6</sup> To verify what effects  $\text{TiO}_2$  capping would have on the dielectric properties, we prepared  $\text{HfSiO}/\text{SiO}_2$  (1.8 nm  $\text{SiO}_2$  thickness) gate stacks as a reference sample 1.

These fabricated gate stacks were examined using SCM measurements in a vacuum ( $10^{-4}$  Pa) at room temperature. The detailed setups of our SCM using the quartz oscillator were described in a previous study.<sup>7,8</sup> Our SCM yielded simultaneous images of the topography and distance differential capacitance ( $dC/dZ$ ). The  $dC/dZ$  signal sensed the static capacitance of the nanometric MOS structure formed by the SCM probe tip, surface oxides, and  $p$ -Si substrate.<sup>8</sup>

In the studies presented here, localized regions within the gate stacks were electrically stressed. A 500-nm-square area was initially stressed by scanning the probe tip while applying positive or negative bias ( $V_{dc}$ ) to the sample's back electrode. Then, the scan area was increased to 1  $\mu\text{m}$  square and the  $V_{dc}$  was reduced to 0 V to image the stressed center area along with the surrounding unstressed regions. The results of this experiment are shown in Fig. 1, which has pairs of simultaneously obtained topographic and  $dC/dZ$  images. Each image pair shows sample 1 [(a) and (b)], 2 [(c) and (d)], and 3 [(e) and (f)] after being initially stressed at a  $V_{dc}$  of +3 V. As can be seen from the topographic images in Figs. 1(a), 1(c), and 1(e), there are no apparent topographic anomalies in the bias-stressed region. The surface roughness of all samples was almost the same and lower than 0.12 nm in terms of the rms value. However, all  $dC/dZ$  images in Figs. 1(b), 1(d), and 1(f) has distinctive bright contrast area corresponding to the bias-stressed region.

<sup>a)</sup>Also at Nanoelectronics Research Institute, National Institute of Advanced Industrial Science and Technology (AIST), Umezono 1-1-1, Tsukuba, Ibaraki 305-8568, Japan. Electronic mail: yu-naitou@aist.go.jp.

<sup>b)</sup>Also at Canon Anelva Corporation, 2-5-1 Kurigi, Asao-ku, Kawasaki 215-8550, Japan.

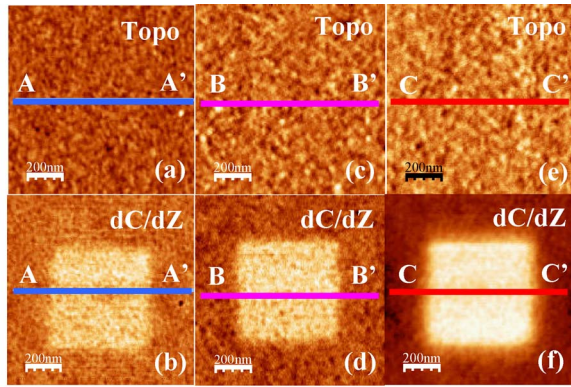


FIG. 1. (Color online) Topography and corresponding  $dC/dZ$  images of samples 1 (reference HfSiO/SiO<sub>2</sub> gate stacks), 2 (TiO<sub>2</sub>/HfSiO/SiO<sub>2</sub> gate stacks annealed at 400 °C), and 3 (TiO<sub>2</sub>/HfSiO/SiO<sub>2</sub> gate stacks annealed at 600 °C) after positive bias stressing. (a) Topography of sample 1, (b)  $dC/dZ$  of sample 1, (c) topography of sample 2, (d)  $dC/dZ$  of sample 2, (e) topography of sample 3, and (f)  $dC/dZ$  of sample 3. Each pair, (a) and (b), (c) and (d), and (e) and (f) were simultaneously scanned. Measurement parameters: stressing bias = +3 V, stressed regions were 500 × 500 nm, scanning areas were 1 × 1 μm, oscillation amplitude of SCM probe tip = 2 nm<sub>p-p</sub>, dc offset bias ( $V_{dc}$ ) = 0 V, and feedback setpoint ( $\Delta f$ ) = +100 mHz.

The effect of bias stressing on the surface morphology and  $dC/dZ$  images can clearly be assessed by inspecting the cross-sectional cuts along the A-A' line [Figs. 1(a) and 1(b)], B-B' [(c) and (d)], and C-C' [(e) and (f)]. The topographic and  $dC/dZ$ -signal profiles along these lines are summarized in Figs. 2(a) and 2(b). No intrinsic topographic changes could be observed between the stressed and unstressed regions in any of the samples, as confirmed by Fig. 2(a). The corresponding  $dC/dZ$ -signal profiles in Fig. 2(b), on the other hand, indicate a clear increment in the  $dC/dZ$ -signal value within the stressed regions. In the same way, Figs. 2(c) and 2(d) show a series of topographic and  $dC/dZ$ -signal profiles for sample 1, 2, and 3 under bias stressing with  $V_{dc} = -3$  V. Similar to the previous results, none of the topographic profiles in Fig. 2(c) indicate obvious differences between stressed and unstressed regions. However, the corre-

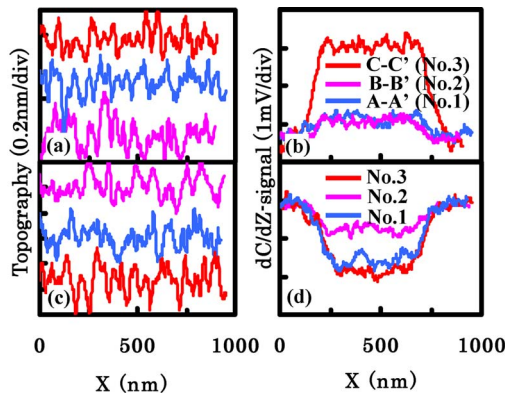


FIG. 2. (Color online) Cross-sectional profiles of bias-stressed topography and corresponding  $dC/dZ$  images. (a) and (b) are results for positive bias stressing, and (c) and (d) are derived from negative bias stressed images. Same color in each profile corresponds to same sample. (a) Topography profiles along line A-A' of Fig. 1(a) (blue), B-B' of Fig. 1(c) (pink), and C-C' of Fig. 1(e) (red). (b)  $dC/dZ$ -signal profiles along line A-A' of Fig. 1(b) (blue), B-B' of Fig. 1(d) (pink), and C-C' of Fig. 1(f) (red). (c) Topography, and (d) corresponding  $dC/dZ$ -signal profiles of samples 1 (blue), 2 (pink), and 3 (red).

sponding  $dC/dZ$ -signal value indicates a reduction within the stressed region, as shown in Fig. 2(d).

There are two important implications to consider the observed dependence of the SCM images on the bias stressing. Positive sample bias stressing induces an increase in the  $dC/dZ$  signal, and negative bias stressing makes the  $dC/dZ$  signal decrease. Second, no changes in the surface topography were observed in the positive or negative bias stressed regions of any of the samples. These two facts indicate that the observed changes in the  $dC/dZ$ -signal profiles by bias stressing were certainly due to electrical effects, and not due to the local oxidation or surface abrasion of high- $k$  films. These stress-induced changes in the  $dC/dZ$  signal also depend on the samples. For positive bias stressing, the increment in the  $dC/dZ$ -signal value between stressed and unstressed regions was  $\sim 2$  mV for sample 3 (annealed at 600 °C), which is larger than that for the two other samples [ $\sim 0.5$  mV for sample 1 (reference) and sample 2 (annealed at 400 °C)], as shown in Fig. 2(b). For negative bias stressing, the decrease in the  $dC/dZ$ -signal value between stressed and unstressed regions was  $\sim 0.8$  mV for sample 2, which is smaller than that for the other two samples ( $\sim 1.8$  mV for samples 1 and 3), as shown in Fig. 2(d).

The possible charge transfer between the metal probe tip and high- $k$  samples by applying positive or negative sample bias are two ways: under positive bias applied, electrons are injected from the probe tip to the trap sites within high- $k$  films, or holes provided by the  $p$ -Si substrate are captured in underlayer SiO<sub>2</sub>/Si interface traps. In contrast, trapped electrons are extracted from high- $k$  films to the probe tip, or captured holes are released from the interface traps to the substrate by applying negative sample bias. From the results in Fig. 2(b), we can conclude that electrons are injected from the probe tip to the traps of high- $k$  films by positive bias stressing, and this causes carriers to accumulate within the  $p$ -Si substrate; therefore, the  $dC/dZ$ -signal, value increases within the stressed region. In a similar way, initially trapped electrons within high- $k$  films might be detrapped by negative bias stressing and, thus, the decrease in the  $dC/dZ$ -signal value resulting from carrier depletion within the  $p$ -Si substrate [Fig. 2(d)]. Consequently from our findings in Figs. 1 and 2 together with the macroscopic  $C$ - $V$  characteristics<sup>6</sup> we can deduce the electron trap properties within TiO<sub>2</sub>/HfSiO/SiO<sub>2</sub> gate stacks for each sample. Macroscopic  $C$ - $V$  curves of sample 1 shows almost no flat band voltage ( $V_{FB}$ ) shift; whereas sample 2 indicates a little, and sample 3 exhibits obvious negative  $V_{FB}$  shift. These results mean that the number of positively charged defects in sample 3 is larger than those in samples 1 and 2. Hence, considering the above, the charging polarity of electron traps and filled traps preexisting within samples 1–3 might be positive and neutral, respectively. The possible origin of such electrical defects within high- $k$  films is oxygen vacancies ( $V_O$ )<sup>9,10</sup> which is neutral and is charged ( $V_O^{2+}$ ) by detrapping. Thus, the electron trapping/detrapping properties of samples 2 and 3, as shown in Figs. 2(b) and 2(d), suggest that both number of  $V_O^0$  and  $V_O^{2+}$  have increased by Ti oxidation annealing at 600 °C. From x-ray photoelectron spectroscopy analysis, we verified that conspicuous Ti diffusion from the TiO<sub>2</sub> layer to the SiO<sub>2</sub> underlayer was caused by 600 °C oxidation annealing.<sup>6</sup> Together with this, Ti diffusion might induce oxygen vacancies within the TiO<sub>2</sub>/HfSiO/SiO<sub>2</sub> gate stacks due to high-temperature oxidation annealing. Furthermore, in Fig. 2(d),



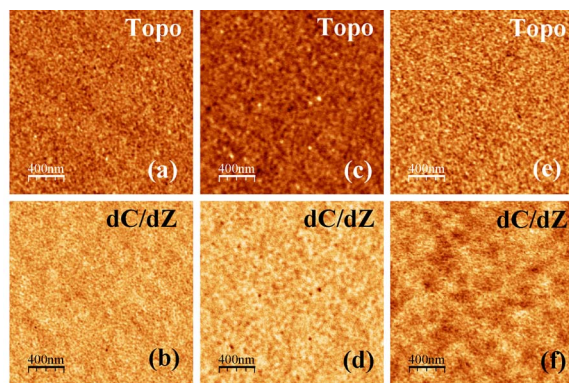


FIG. 3. (Color online) Sets of simultaneously obtained topography and  $dC/dZ$  images of samples 1–3. (a) Topography of sample 1, (b)  $dC/dZ$  of sample 1, (c) topography of sample 2, (d)  $dC/dZ$  of sample 2, (e) topography of sample 3, and (f)  $dC/dZ$  of sample 3. Measurement parameters: scanning areas were  $2 \times 2 \mu\text{m}$ , oscillation amplitude of SCM probe tip  $= 2 \text{ nm}_{p-p}$ , dc offset bias ( $V_{dc}$ )  $= 0 \text{ V}$ , and feedback setpoint ( $\Delta f$ )  $= +100 \text{ mHz}$ .

the decrease in the  $dC/dZ$  signal by negative bias stressing for sample 3 seems to be comparable to that observed for sample 1. Although further studies are required to clarify the detailed mechanism of the microscopic trapping/detrapping phenomena, a possible explanation is as follows. The preexisting positive charges within sample 3 induce electric field whose direction is opposite to the externally applied electric field thereby decreasing effective electric field within the gate stacks during the negative bias stressing. Therefore, in Fig. 2(d), the decrease in the  $dC/dZ$  signal for sample 3 by negative bias stressing should be underestimated by considering the difference of the effective electric field between samples 1 and 3.

Figure 3 show  $2 \mu\text{m}$  square images of  $dC/dZ$  and corresponding topographies of samples 1–3 samples. These images were taken under the same condition of  $V_{dc} = 0 \text{ V}$ . We observed no specific features either in the topographies or  $dC/dZ$  images of sample 1 [Figs. 3(a) and 3(b)] and sample 2 [Figs. 3(c) and 3(d)] samples. However, the  $dC/dZ$  image of sample 3 [Fig. 3(f)] shows a corrugated contrast having no correlation with the corresponding surface topography of Fig. 3(e). Our former studies have revealed that the  $dC/dZ$  signal is not only related to local variations in gate oxide

capacitance ( $C_{ox}$ ), but also to the local depletion capacitance ( $C_{dep}$ ) formed by the probe tip.<sup>8</sup> As the positive fixed charges in the gate stacks increase the carrier depletion layer within the  $p$ -Si substrate just beneath the SCM probe tip, the dark contrasting regions in the  $dC/dZ$  image of Fig. 3(f) can be attributed to the inhomogeneous distribution of positive fixed charges. Furthermore, taking the above discussion into account we can conclude that Ti diffusion within the  $\text{TiO}_2/\text{HfSiO}/\text{SiO}_2$  gate stacks due to high-temperature annealing is not a spatially isotropic phenomenon.

In conclusion, we studied the charge-trapping properties of  $\text{TiO}_2/\text{HfSiO}/\text{SiO}_2$  gate stacks through  $dC/dZ$  imaging by SCM. From an examination of the positive and negative bias stress of gate stacks with different preparation processes, we concluded that there were electron traps and filled traps within the gate stacks. The origin of these charged defects was ascribed to oxygen vacancies, which is caused by the diffusion of Ti during high-temperature annealing. Furthermore, we also found that these charged defects had a spatially inhomogeneous distribution within the gate stacks, indicating that the Ti diffusion was not a spatially isotropic phenomenon.

This study was partially supported by the Industrial Technology Research Grant Program in 2007 from the New Energy and Industrial Technology Development Organization (NEDO) of Japan.

- <sup>1</sup>G. D. Wilk, R. M. Wallace, and J. M. Anthony, J. Appl. Phys. **89**, 5243 (2001).
- <sup>2</sup>B. Govoreanu, P. Blomme, M. Rosmeulen, J. Van Houdt, and K. De Meyer, IEEE Electron Device Lett. **24**, 99 (2003).
- <sup>3</sup>R. B. van Dover, Appl. Phys. Lett. **74**, 3041 (1999).
- <sup>4</sup>K. Torii, A. Aoyama, S. Kamiyama, Y. Tamura, S. Miyazaki, H. Kitajima, and T. Arikado, Tech. Dig. VLSI Symp. **2004**, 112.
- <sup>5</sup>H. Watanabe, S. Horie, T. Minami, N. Kitano, M. Kosuda, T. Shimura, and K. Yasutake, Jpn. J. Appl. Phys., Part 1 **46**, 1910 (2007).
- <sup>6</sup>H. Arimura, S. Horie, Y. Oku, T. Minami, N. Kitano, M. Kosuda, T. Hosoi, T. Shimura, and H. Watanabe, Appl. Surf. Sci. (submitted).
- <sup>7</sup>Y. Naitou and N. Ookubo, Appl. Phys. Lett. **85**, 2131 (2004).
- <sup>8</sup>Y. Naitou, A. Ando, H. Ogiso, S. Kamiyama, Y. Nara, K. Yasutake, and H. Watanabe, J. Appl. Phys. **101**, 083704 (2007).
- <sup>9</sup>K. Shiraishi, K. Yamada, K. Torii, Y. Akasaka, K. Nakajima, M. Konno, T. Chikyow, H. Kitajima and T. Arikado, Jpn. J. Appl. Phys., Part 2 **43**, L1413 (2004).
- <sup>10</sup>J. Robertson, Rep. Prog. Phys. **69**, 327 (2006).